CONF-8710165--4

UCRL- 97801
PREPRINT

Database of Average-Power Damage Thresholds at 1064 nm

F. Rainer,
E. A. Hildum,
D. Milam

This paper was prepared for submittal to
The Boulder Damage Symposium
October 26-28, 1987

December 14, 1987

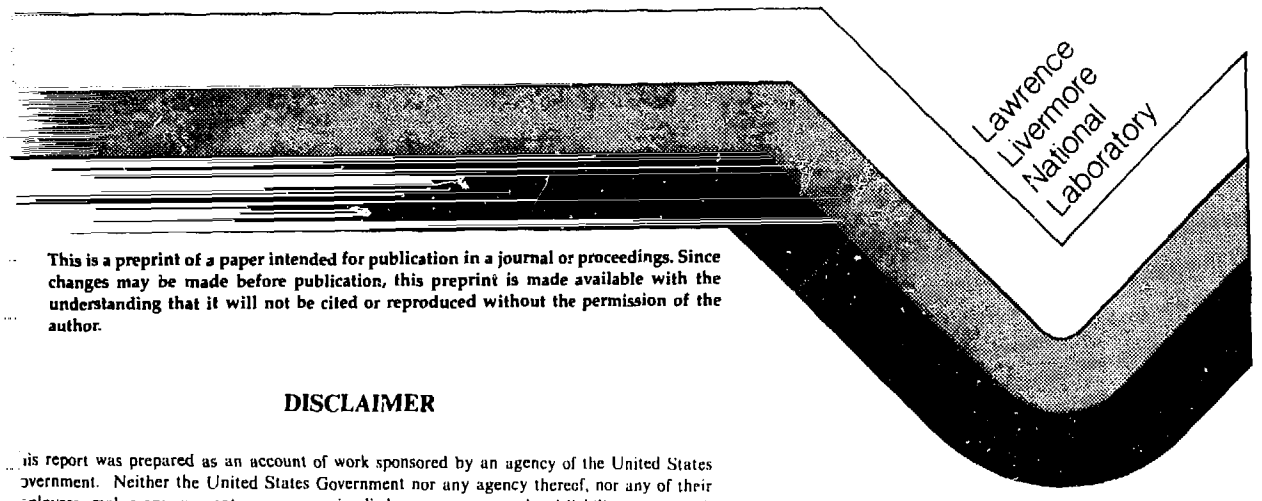

Database of Average-Power Damage Thresholds at 1064 nm*

F. Rainer, E. A. Hildum, and D. Milam

Lawrence Livermore National Laboratory

Livermore, CA 94550

UCRL--97801

DE88 004352

ABSTRACT

We have completed a database of average-power, laser-induced, damage thresholds at 1064 nm on a variety of materials. Measurements were made with a newly constructed laser at the Lawrence Livermore National Laboratory (LLNL) to provide design input for moderate and high average-power laser projects. The measurements were conducted with 16-ns pulses at pulse-repetition frequencies ranging from 6 to 120 Hz. Samples were typically irradiated for times ranging from a fraction of a second up to 5 minutes (36,000 shots). We tested seven categories of samples which included antireflective coatings, high reflectors, polarizers, single and multiple layers of the same material, bare and overcoated metal surfaces, bare polished surfaces, and bulk materials. The measured damage thresholds ranged from < 1 J/cm^2 for some metals to > 46 J/cm^2 for a bare polished glass substrate.

Key words: antireflective coatings; bare substrates; bulk damage; damage; e-beam coatings; laser-induced damage; metallic coatings; polarizers; reflectors; sol-gel coatings; thin films.

*Work performed under the auspices of the U. S. Department of Energy by Lawrence Livermore National Laboratory under Contract No. W-7405-ENG-48.

1. Introduction

We have constructed the REPTILE (Repetition Laser Experiment) Facility to conduct laser-induced damage studies on a variety of material types at moderate pulse-repetition frequencies (PRF) ranging up to 120 Hz at 1064 nm. The facility supports the development of damage resistant materials needed for several laser projects at the Lawrence Livermore National Laboratory. It supplements our data gathering capabilities at low PRF from our single-shot damage-test facilities, and provides an efficient means to conduct the following types of tests: PRF dependent studies, thermal accumulation effects, N-on-1 irradiations, lifetime tests, and large area scans. Details of the facility design and computer control system are presented in a companion paper at these proceedings.[1]

2. Laser parameters at the sample plane

The pulses from four commercial YAG lasers, each operating at 30 Hz, are interleaved to yield PRF's up to 120 Hz. At the sample plane we obtain pulse energies up to 0.6 J with peak fluences > 40 J/cm^2. The spatial profile is nominally Gaussian with spot sizes adjusted to be typically 0.5 to 1.0 mm diameter FWHM. Peak fluence can be controlled by varying the spot size and/or by ejecting a fraction of the beam energy with a polarizer-waveplate pair. The output polarization can be set to alternate between S and P from pulse to pulse, or remain fixed at any orientation of linear polarization. The average energy of the four lasers is monitored by a calorimeter. Individual laser pulse energies are measured with a PIN diode which is calibrated with the calorimeter. We use a computer to generate a histogram of pulse energy distributions for each laser and calculate peak fluences either by means of apertured

calorimetry or by integrating the spatial profile obtained from a CID video camera at the sample plane. The profile is displayed in a false color format on a TV monitor. We take the average of all peak fluence calculations for all four lasers to yield a peak fluence value for a particular irradiation interval. A second PIN diode measures the temporal profile.

3. Sample diagnostics and irradiation conditions

We examine the test samples for damage by comparing pre- and post-irradiation photographs generated by Nomarski, bright field or dark field microscopy at typical magnifications of 100. These techniques have been described extensively at previous Boulder Damage Symposia and elsewhere. [2] We also monitor the accumulation of heat on the sample surface by means of an infrared imaging camera which can resolve temperature rises of 0.1° C in spatial elements nominally 0.2 mm square.

Most tests were conducted at a PRF of 120 Hz. However, until we implemented a technique for combining the total energy of each of the four lasers into one collinear beam, irradiations at relatively high fluence or with single linear polarization were limited to a maximum PRF of 60 Hz. For instance, all polarizers and high-threshold bare substrates were irradiated at 60 Hz. For isolated instances, we also conducted tests at PRF's ranging from 6 to 30 Hz to compare PRF effects. Our standard procedure was to irradiate a fixed site on the sample for up to five minutes (36,000 shots) before examining it again for damage. We interrupted the irradiation if obvious damage was observed, typically manifested by a plasma, by the emission of coating debris (often

accompanied by considerable noise), or by increased scatter of light from a collinear He-Ne laser beam. About 10 sites were irradiated at different fluences to establish a damage threshold fluence, defined to be the mean between the highest non-damaging fluence and the lowest damaging fluence. In some circumstances we scanned the sample continuously through the irradiating beam, usually at about 0.1 mm/min, and then conducted scanned microscopy after the irradiation scan was completed. Our samples were usually mounted at 10° incidence to the input beam to avoid interference effects from rear surface reflections. Polarizers and some special reflectors were tested at their design angles which ranged up to 66°.

4. Databases of laser damage thresholds

4.1 General observations

We conducted over 200 damage tests on samples in seven different categories. These were supplied to us by more than 20 sources both from within LLNL and from commercial vendors. Our databases contained results from a broad spectrum of samples representing state of the art technology, current optics in use on one of the laboratory's laser systems, and both current and old developmental research samples. None of the results of the individual categories of databases is necessarily representative of the highest, lowest or average damage thresholds attainable within that category. Moreover, in some cases they represent evolutionary development of improved thresholds or parameter studies, which may encompass a large spread in thresholds.

Half way through our test program we installed an infrared imaging camera to observe the accumulation of heat on the irradiated sample under PRF conditions. To first order, we found no discernible difference in sample thresholds between those measured at 120 Hz and lower PRF's. In general we found that there was very little macroscopically observable sample heating. Temperature changes were usually on the order of a few tenths of a degree Celsius. As expected, partially absorbing bulk materials yielded the highest surface temperature rises, usually no more than 4° C. Since the smallest resolving element of the camera was about 0.2 mm square, probable heating of micron-sized defects from which damage often originated was not resolvable. Typically, damage occurred within the first fraction of a second of irradiation, although observable damage was sometimes delayed by as long as ?35 seconds after the start of irradiation. Catastrophic failure, either delayed or early, usually produced a plasma with temperature of hundreds of degrees. The camera, however, reads a time-averaged temperature which vastly underestimates the short-lived maximum temperature in the plasma.

4.2 Antireflective (AR) coatings

A typical database comparing e-beam-deposited and sol-gel-fabricated coatings is shown in Fig. 1. The histograms display the number of samples that were tested whose damage thresholds fell within a given window 2-J/cm^2 wide. The e-beam coatings were a variety of multi-layer coating designs deposited on either fused silica or BK-7. We further categorize the samples by material used for the high index-of-refraction layers. The low-index materials were either silica or magnesium

fluoride. The best AR was a tantala/silica stack, but then, so was the worst. The large spread in thresholds is attributable to variations in coating design and deposition parameters. This threshold distribution, as well as those that follow can obviously be skewed at will by further tests of particular designs. Therefore, tests of more samples of the optimum design for each material combination would yield tighter distribution groupings for tantala, zirconia and titania based AR's.

The sol-gel AR's are single- and multiple-layer porous coatings of the one material noted, primarily silica. These were deposited at LLNL by a variety of processing techniques to establish the optimum parameters for producing high damage threshold AR's. The spread in silica thresholds represents improvements in the deposition process rather than intrinsic variability in the sol-gel process. In addition, these coatings were deposited on either fused silica, calcium fluoride or KDP crystals. The lowest silica thresholds were those on KDP which did not have particularly clean or well polished surfaces. In general we found that the optimally deposited sol-gel AR's had thresholds comparable to the best e-beam deposited coatings.

4.3 Highly reflective (HR) coatings

We tested 32 HR coatings of greatly varied coating designs. These are shown in Fig. 2. Four different vendors supplied e-beam-deposited HR's on fused silica, BK-7, SiC, or Cu substrates. The low-index material for each sample was silica, although for four samples the vendors did not disclose the constituent materials. Because the number of samples for each material combination is relatively low, and parameter and vendor variations are large, it would be imprudent to discount any

material combination based on these tests. The highest threshold sample was a titania/silica stack developed as a research coating several years ago. Most of the other titania/silica coatings were variations of the optimum design so that gaps in the distribution could readily be filled by selecting different HR designs. Samples which had high damage thresholds when measured with single, 1-ns pulses several years ago still had correspondingly high thresholds under our current PRF conditions.

All of the sol-gel HR coatings were fabricated at LLNL and consisted of multiple-layer stacks of the materials listed alternating with sol-gel-deposited silica layers. All were deposited on fused silica substrates. As will be shown later, all of these coatings had thresholds notably lower than those of single or multiple layers of the individual constituent materials. Contrasted with AR designs tested, the sol-gel HR's failed to yield thresholds comparable to the best e-beam HR's. In particular, it can be noted that some of the best e-beam HR coatings were titania/silica combinations, whereas these combinations with sol-gel processing had some of the lowest thresholds.

4.4 Polarizers

Our tests include 33 damage threshold measurements of e-beam and sol-gel deposited polarizers shown in Fig. 3. All but two tests were conducted at 60 Hz. Each sample was irradiated at its optimum design angle of incidence which ranged from 55° to 66°. Seven different vendors supplied e-beam deposited polarizers, although not all provided information on the coating design or the constituent materials. All of the designs provided were multi-layer stacks of silica and the high-index

materials identified in the figure. The identified substrates were either fused silica or BK-7. Most of the tests were conducted with P-polarized pulses. However, six samples were also tested at the same angle of incidence with S-polarization irradiation. Of these we noted that the S-polarization threshold was 20% lower for two samples, identical for another two, and indeterminate for the remaining two. As with our HR tests, we must emphasize that the database is too small to exclude any material combination from high threshold polarizer designs. Typically we found polarizers to have a higher density of coating defects than HR's but only a small fraction of the defects actually proved to be the source of damage. Once damage was initiated we found a greater tendency for both the magnitude and number of damage points to grow. The highest thresholds were obtained from research grade hafnia/silica combinations.

All of the sol-gel polarizers were single-layer coatings fabricated on fused silica substrates for process development at LLNL. Although sol-gel coatings were exceptionally clean in comparison with the e-beam-coated polarizers, damage accumulated similarly with successive irradiations. Damage to the titania samples grew particularly rapidly with successive shots compared to the tantala samples. For the limited number of tantala and titania polarizers tested we found thresholds to be comparable to their e-beam material counterparts. However, the degree of polarization in the sol-gel samples is not optimum and is obtained only at high angles of incidence, up to 66°. Only one sample was tested at both P- and S-polarization with a 16% drop in threshold for the latter.

4.5 Single and multiple layers of a single material

All single material tests were conducted with LLNL-fabricated sol-gel coatings on fused silica substrates. We tested 51 samples which are detailed in Fig. 4. The highest thresholds were obtained from alumina coatings although zirconia, hafnia, and tantala coatings also yielded promising thresholds. The two silica coatings were special designs to produce a frosted surface effect. Otherwise, silica coatings, previously listed as AR's, had thresholds comparable to those of aluminas. Possibly because of the extra handling involved, multi-layer coatings made by alternating different materials had lower thresholds than those of the individual constituent materials. We conducted no specific tests to see if the same effect applied to multiple layers of the same material. With these, as with other sol-gel coatings, we often observed a faint emission of white light from the surface for the first fraction of a second of irradiation. We conclude that this is produced by the combustion of residual solvent trapped in the outer portion of these porous coatings. Post-irradiation microscopy showed no evidence of damage in these situations. This shows that light emission from an irradiated sample is not a conclusive indicator of coating damage.

4.6 Bare and overcoated metals

We have examined a limited number of different metallic surfaces which were either plated on substrates or were formed by polishing or diamond-turning bare metal substrates. In addition, most of the samples also had e-beam deposited dielectric coatings to form either a protective layer or a dielectric HR. The results of 17 damage tests on samples supplied by eight different vendors are summarized in Fig. 5. The

variety in metals, surface preparation, coatings, vendors, and handling history makes it difficult to note more than a few superficial observations. The highest threshold was 4.3 J/cm^2 for a diamond-turned copper substrate with a dielectric HR stack, yet a comparable sample had a notably lower threshold. All other metals had thresholds of 2 J/cm^2 or less. Molybdenum and copper mirrors which had no dielectric overcoats or HR's fared worse than their counterparts with dielectric coatings. We found in all cases that damage was highly dependent on existing observable artifacts. Under threshold level irradiation damage nucleated at these artifacts but did not grow with repeated irradiation. However, a slight increase in fluence typically caused massive damage. Slow heat accumulation, on the order of 2-3° C over a span of a few minutes, was observed with the infrared camera. However, the temperature of micron-sized artifacts was not resolvable. Basically, all of the metallic samples had among the lowest thresholds of the various categories tested.

4.7 Bare polished surfaces

We conducted damage tests on four categories of non-metallic bare polished substrates: fused silica, calcium fluoride, non-linear crystals and silicon carbide (Fig. 6). Besides actual differences in materials, other factors influencing the level and spread in damage thresholds of these materials are the quality of polishing or surface preparation and the degree of handling prior to testing. Two thirds of the threshold measurements are for exit-surface irradiation. Rear-surface damage is both easily detected and the more likely failure mode for a bare, highly transparent substrate irradiated at near normal incidence. [3]

Unsurprisingly, the highest thresholds were obtained for fused silica, ranging from 25.3 to > 46 J/cm^2. In several cases, limitations on available fluence prevented us from inducing any damage at all. We found no degradation to damage thresholds when the fused silica was subjected to final figuring by ion milling. [4] Among the non-linear crystals tested were KDP, KD*P and LAP (l-arginine phosphate). All exhibited large-area temperature rises of 3-5° C with damage occurring 3-235 seconds after the start of irradiation. Polishing differences, rather than material type, appeared to be the dominant factor in damage level.

4.8 Bulk materials

Many of the materials used in the bare surface tests were also examined for damage within the bulk material itself (Fig. 7). Bulk damage was usually first detected by increased scattering of light from a collinear He-Ne laser beam. This was followed by more detailed microscopy through the bulk of the substrate. It was occasionally difficult to differentiate between rear surface and bulk damage when massive damage propagated quickly from near the rear surface into the bulk with repeated irradiation. For the non-linear materials, the threshold for isolated bulk damage was typically 30% lower than the threshold for surface damage. In the calcium fluoride crystals, the threshold for surface pitting was less than that for bulk damage which was not observed except in instances where surface pitting grew under repeated irradiation and propagated into the bulk. We list both an indeterminate threshold and number of tests for fused silica. We conducted many tests of bare and AR coated samples for which we were never able to induce bulk damage at fluences exceeding 36 J/cm^2.

4.9 Summary

In table 1, we summarize the results of all damage tests conducted with the REPTILE facility to date. We list the maximum, median and minimum thresholds obtained within each sample category, but stress that the threshold distribution can be skewed readily by the choice of samples selected for testing. The reported tests were neither exhaustive nor systematic and are not necessarily indicative of the potentials for materials or designs.

5. Conclusions

A database of laser-induced damage thresholds of seven categories of samples, comprising more than 200 tests, was compiled on the REPTILE Damage Test Facility. The tests were conducted with 16-ns, 1064-nm pulses at PRF's ranging from 6 to 120 Hz. Although often including only a minimal number of samples, the individual databases provide rudimentary guidelines on the status of thresholds of currently available optics. Highest thresholds were obtained for clean well-polished fused silicas whose thresholds for both bulk and surface damage readily exceeded 36 J/cm^2. Non-linear crystals that we tested were limited by their bulk damage thresholds although they had relatively poorly polished surfaces. Optimized deposition for both e-beam and sol-gel AR coatings yielded thresholds of 30 to 35 J/cm^2. The best research-grade, e-beam-deposited, HR coatings also achieved high thresholds up to 36 J/cm^2. However, most e-beam HR's and all sol-gel HR's achieved, at best, only half that level. Probably because polarizers are usually more complex coatings requiring more handling, they had somewhat lower thresholds than comparable HR coatings. During the development of many

of the above sol-gel coatings we tested many single- or multiple-layer sol-gel films of only one material. In general we found that their individual high thresholds were not attained when combined with other materials to produce coating stacks. Lowest in threshold of all the categories tested were metallic coatings. Even with otherwise good quality e-beam deposited HR stacks deposited over them, metallic coatings failed to yield thresholds higher than 4.3 J/cm^2.

One of our principal goals with REPTILE was to determine if PRF effects would come into play at or below 120 Hz. Although we did encounter samples which took up to several minutes to fail catastrophically, microscopic damage was usually already evident from the first fraction of a second of irradiation. Moreover, we found no significant difference in thresholds between PRF data measured on REPTILE versus single-shot thresholds at the same pulse duration from other damage facilities. We detected negligible heat accumulation in our samples over the course of five minutes of irradiation. However, we cannot rule out possible thermal effects due to unresolvable micron-sized defects.

In general we found REPTILE to provide a very flexible means of producing definitive thresholds with a rapid turnaround. In particular, it has proved to be especially effective for both lifetime and large area damage test irradiations.

6. References

[1] Hildum, E. A.; Rainer, F; Milam, D. A new average-power damage test facility at LLNL. Boulder Damage Symposium. 1987, October 26-28.

[2] Rainer, F.; Deaton, T. F. Laser damage at short wavelengths. Appl. Opt. 21(10); 1722-1724; 1982 May 15.

[3] Crisp, M. D.; Boling, N. L.; Dube, G. Importance of Fresnel reflections in laser surface damage of transparent dielectrics. Appl. Phys. Lett. 21; 364-366; 1980.

[4] Wilson, S. R.; Reicher, D. W.; McNeil, J. R.; McNally, J. J.; Milam, D.; Gonzales, R.; Rainer, F. Laser damage studies of ion milled fused silica. Boulder Damage Symposium. 1987, October 26-28.

Table 1. Summary of Laser Damage Thresholds
1064-nm, 16-ns Pulses at 6-120 Hz

Category	Type	# of Tests	Threshold (J/cm^2) Max.	Median	Min.
AR	E-beam, sol-gel	33	35	18	5
HR	E-beam, sol-gel	32	>36	9	1
Polarizer	E-beam, sol-gel	33	>23	8	1
Single layer	Sol-gel	51	32	13	1
Metal	Polished, turned, plated, coated	17	4	1	<1
Bare surface	Polished, milled, etched	29	>46	25	2
Bulk material	Silicas, fluorides, crystals	>13	>36	>14	9

Figure Captions

1. Distribution of laser damage thresholds of 33 e-beam- and sol-gel-deposited anti-reflective coatings. Spreads in the threshold for a particular material combination are attributable to different coating designs or deposition parameters.
2. Laser damage thresholds of 32 e-beam- and sol-gel-deposited highly reflective coatings. All samples are comprised of multi-layer stacks of the designated high-index material and silica. Materials of some e-beam coatings were not specified by the vendors.
3. Laser damage thresholds of 33 e-beam and sol-gel deposited polarizers. Except for those listed as unknown, all e-beam deposited polarizers consisted of multi-layer stacks of the materials listed plus silica. The sol-gel polarizers were all single layer coatings.
4. Laser damage thresholds of 51 single and multiple-layer sol-gel samples of a single material. All were fabricated at LLNL on fused silica substrates. The two silica tests were for frosted type coatings. All other silica tests are listed under the AR database.
5. Laser damage thresholds of 17 metallic reflectors from 8 vendors. The metal surface preparation was by diamond turning (D), electroplating (E), or polishing (P). Some samples had dielectric overcoats of a few layers (OC) or a full high reflector stack (HR).
6. Laser induced damage thresholds of 29 bare polished, ion-milled, or etched surfaces of dielectric substrates. Measurements were made both on the entrance and exit surfaces.

7. Laser induced damage thresholds of bulk materials. Damage was readily observed in non-linear crystals at fluences averaging 30% less than surface thresholds. No damage was observed in calcium fluoride before massive damage from the rear surface propagated into the bulk material. No bulk damage was observed in any fused silica sample at fluences exceeding 36 J/cm^2.

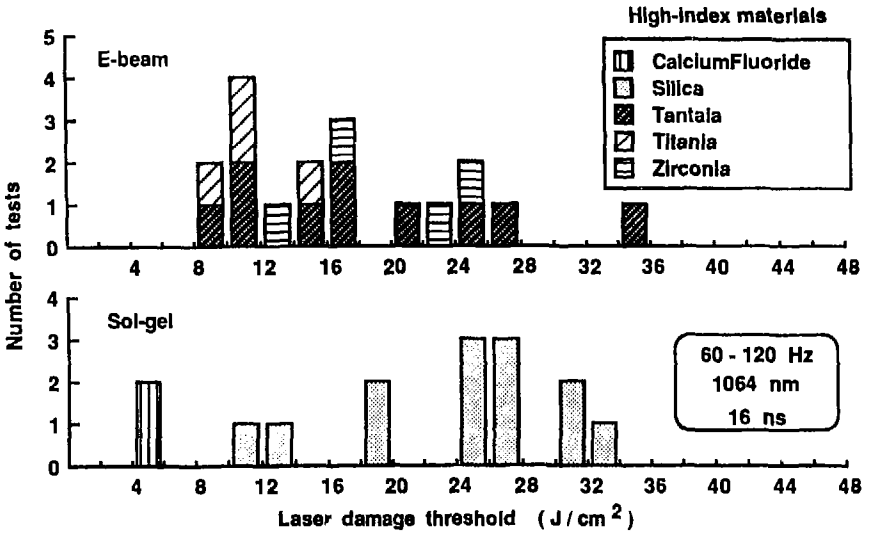

Figure 1

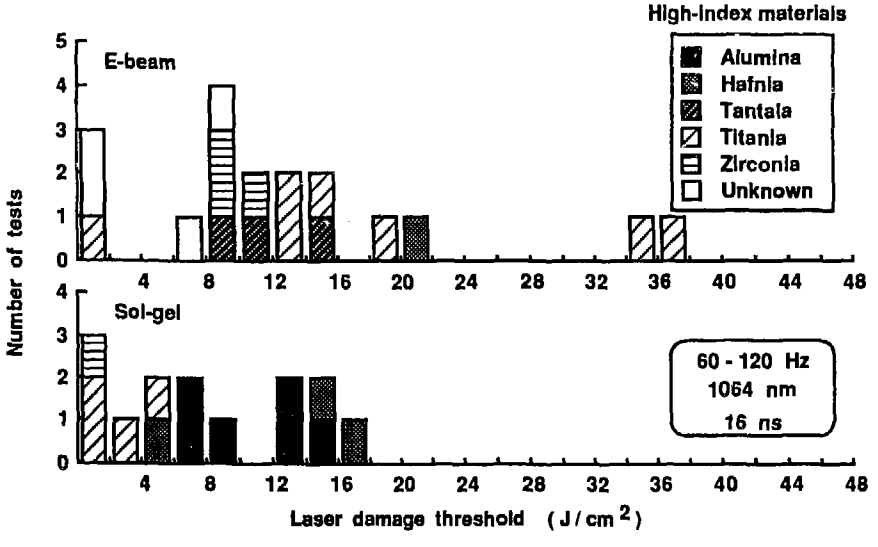

Figure 2

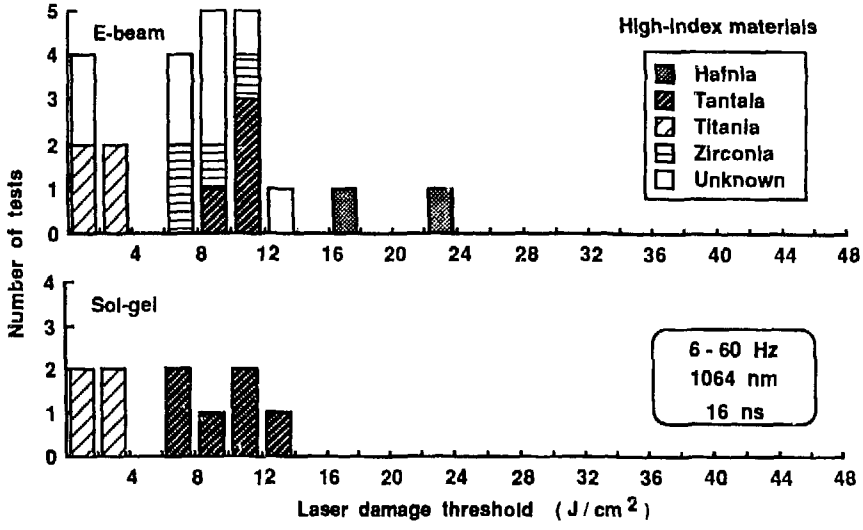

Figure 3

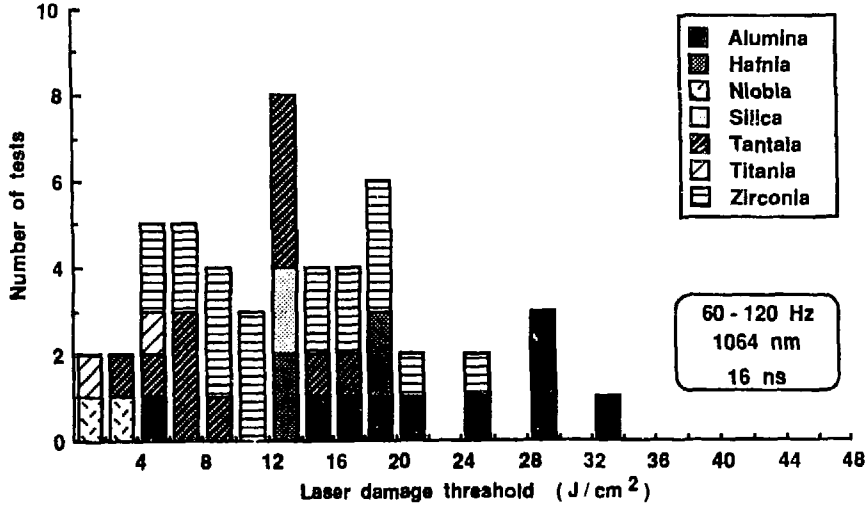

Figure 4

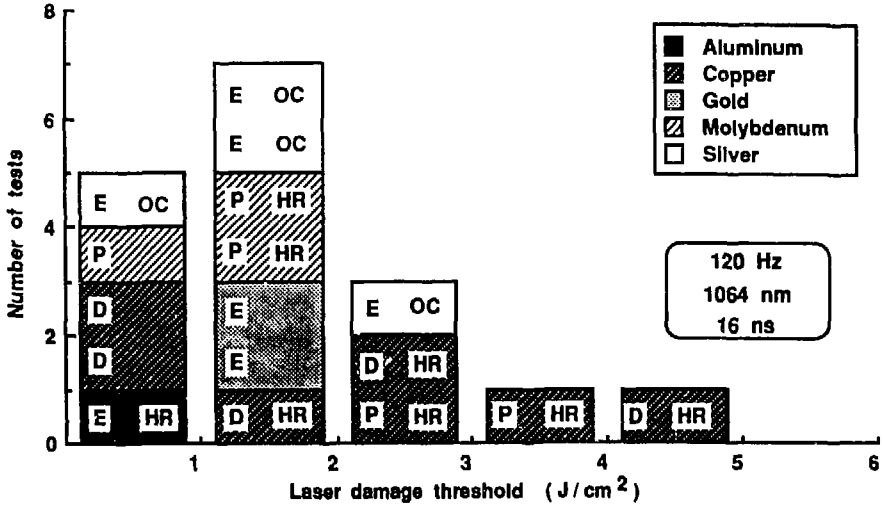

Figure 5

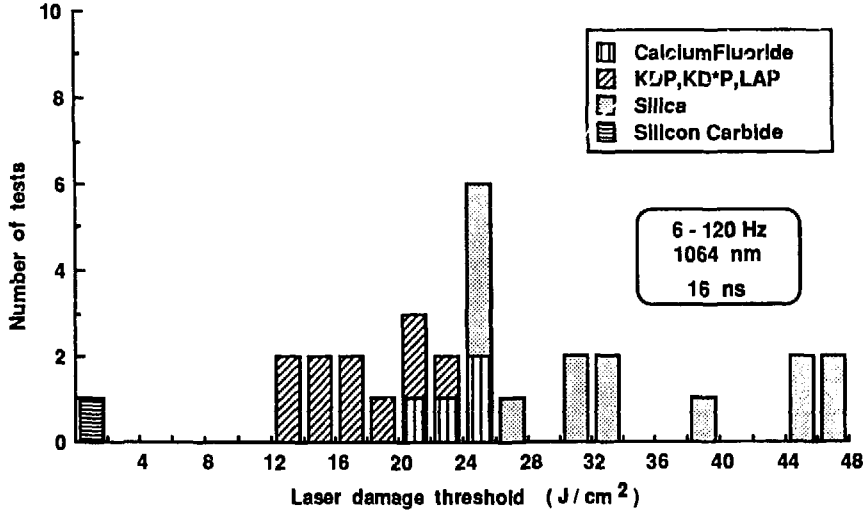

Figure 6

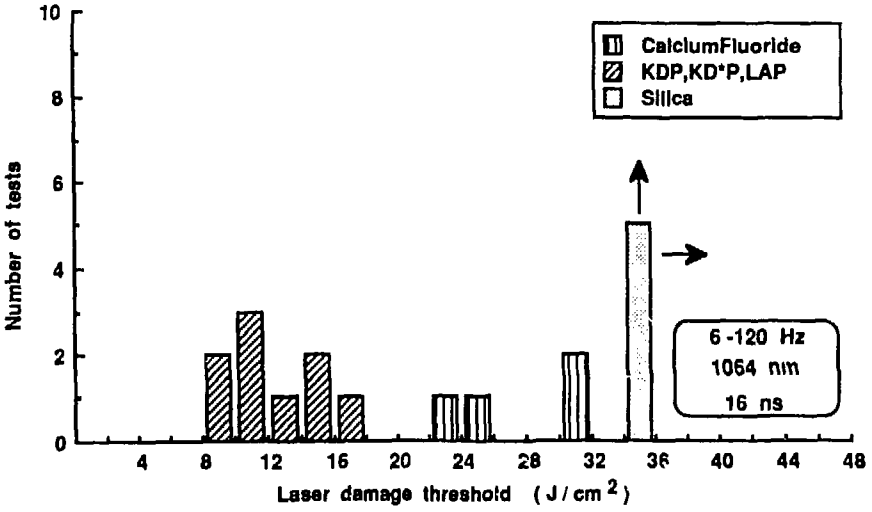
CalciumFluoride
KDP,KD*P,LAP
Silica
6-120 Hz
1064 nm
16 ns
Number of tests
Laser damage threshold (J/cm 2)
0
2
4
6
8
10
4
8
12
16
20
24
28
32
36
40
44
48

Figure 7